12-4-2010

Radiative Forcing Over the Conterminous United States Due to Contemporary Land Cover Use Change and Sensitivity to Snow and Interannual Albedo Variability

Christoper A. Barnes
South Dakota State University

David P. Roy
South Dakota State University, david.roy@sdstate.edu

Recommended Citation
Barnes, C. A., and D. P. Roy (2010), Radiative forcing over the conterminous United States due to contemporary land cover land use change and sensitivity to snow and interannual albedo variability, J. Geophys. Res., 115, G04033, doi:10.1029/2010JG001428.

Radiative forcing over the conterminous United States due to contemporary land cover land use change and sensitivity to snow and interannual albedo variability

Christopher A. Barnes[1] and David P. Roy[1]

Received 10 May 2010; revised 17 August 2010; accepted 7 September 2010; published 4 December 2010.

[1] Satellite-derived land cover land use (LCLU), snow and albedo data, and incoming surface solar radiation reanalysis data were used to study the impact of LCLU change from 1973 to 2000 on surface albedo and radiative forcing for 58 ecoregions covering 69% of the conterminous United States. A net positive surface radiative forcing (i.e., warming) of 0.029 Wm^{-2} due to LCLU albedo change from 1973 to 2000 was estimated. The forcings for individual ecoregions were similar in magnitude to current global forcing estimates, with the most negative forcing (as low as -0.367 Wm^{-2}) due to the transition to forest and the most positive forcing (up to 0.337 Wm^{-2}) due to the conversion to grass/shrub. Snow exacerbated both negative and positive forcing for LCLU transitions between snow-hiding and snow-revealing LCLU classes. The surface radiative forcing estimates were highly sensitive to snow-free interannual albedo variability that had a percent average monthly variation from 1.6% to 4.3% across the ecoregions. The results described in this paper enhance our understanding of contemporary LCLU change on surface radiative forcing and suggest that future forcing estimates should model snow and interannual albedo variation.

Citation: Barnes, C. A., and D. P. Roy (2010), Radiative forcing over the conterminous United States due to contemporary land cover land use change and sensitivity to snow and interannual albedo variability, *J. Geophys. Res.*, *115*, G04033, doi:10.1029/2010JG001428.

1. Introduction

[2] Surface albedo affects the Earth's radiative budget by controlling how much incoming solar radiation is absorbed and reflected by the Earth's surface and is a fundamental parameter for characterizing the Earth's radiative regime [*Dickinson*, 1995]. It is thought that land cover land use (LCLU) change during the 20th century, primarily increasing croplands and pastures and decreasing forested land [*Ramankutty and Foley*, 1999], has resulted in a global net cooling of approximately -0.25 Wm^{-2} [*Intergovernmental Panel on Climate Change* (*IPCC*), 2007]. Changes in surface albedo depend on both the type and spatial extent of LCLU change and the spatial averaging of opposite signs of LCLU induced radiative forcing may under represent LCLU contributions over large areas [*Pielke et al.*, 2002; *Kleidon*, 2006; *Barnes and Roy*, 2008]. Surface albedos vary seasonally because of factors including land management practices and phenology [*Gao et al.*, 2005] and failure to adequately prescribe seasonal vegetation variations may significantly bias LCLU change forcing estimates [*Nair et al.*, 2007]. Similarly, snow is temporally variable, and because the albedo of snow is high relative to that of vegetation and soil, changes from snow-hiding to snow-revealing LCLU types may have a significant surface radiative forcing effect [*Betts*, 2000].

[3] In this paper we update earlier work [*Barnes and Roy*, 2008] to quantify the surface radiative forcing due to contemporary LCLU albedo change (1973–2000) for the conterminous United States (CONUS) using spatially and temporally explicit satellite-derived LCLU change and albedo data. We provide a revised estimate of the CONUS surface radiative forcing by considering a greater area, 69% of the CONUS, and by improving the representation of the LCLU class albedos. Median monthly snow and snow-free albedo climatology values are derived from 9 years of Moderate Resolution Imaging Spectroradiometer (MODIS) albedo product data for 10 LCLU classes in 58 ecoregions. These, and monthly surface solar radiation, monthly snow fraction, and 1973–2000 LCLU change data, are used to compute monthly and annual ecoregion forcing estimates.

[4] The sensitivity of the forcing estimates to interannual albedo variations that are not associated with LCLU change are examined. Although interannual albedo variability is usually lower than seasonal variability [*Wang et al.*, 2004; *Gao et al.*, 2005; *Matsui et al.*, 2007], it is unknown if albedo changes from 1 year to another significantly impact LCLU albedo change forcing estimates. In addition, by incorporating spatially and temporally explicit snow albedo

[1]Geographical Information Science Center of Excellence, South Dakota State University, Brookings, South Dakota, USA.

0148-0227/10/2010JG001428

Table 1. The 10 Land Cover Land Use Classes Defined in the Decadal Conterminous United States Landsat Classifications[a]

LCLU Class	CONUS Snow-Free Albedo	CONUS Snow Albedo
Barren	0.194	0.486 (2)
Agriculture	0.169	0.567 (1)
Mining	0.157	0.442 (5)
Developed	0.157	0.415 (7)
Grass/shrub	0.156	0.456 (4)
Wetland	0.142	0.465 (3)
Mechanically disturbed	0.139	0.315 (9)
Nonechanically disturbed	0.130	0.432 (6)
Forest	0.130	0.243 (10)
Water	0.075	0.346 (8)

[a]Corresponding CONUS estimates of the annual snow and snow-free broadband white-sky MODIS albedo values are tabulated for each class. The LCLU classes are ranked in descending snow-free albedo order. The rank of the snow albedos is denoted in brackets in the third column. The LCLU class albedos are shown here for interpretive purposes only; they were not used in the described analyses. The albedos were computed for each class i from all the valid MODIS albedo samples for each month m (1…12), ecoregion e (Figure 1), and year y (2000–2009) as

$$\text{CONUS } \alpha_i = \underset{12\text{ months}}{\text{median}}\left\{ \underset{58\text{ ecoregions}}{\text{median}}\left\{ \underset{9\text{ years}}{\text{median}}\left\{\alpha_{i,m,e,y}\right\}\right\}\right\}.$$

data, we examine what impact modeling snow conditions has on contemporary LCLU albedo change surface radiative forcing, particularly in the northern and high-altitude snow-prone regions of the CONUS.

2. Study Area and Data

[5] The LCLU information for the CONUS are currently being generated from decadal Landsat data (1973–2000) at the United States Geological Survey (USGS) Earth Resources Observation and Science (EROS) Center [*Loveland et al.*, 2002; P. Jellison and W. Acevedo, USGS Land Cover Trends Project, unpublished data, 2010]. Landsat multispectral scanner, thematic mapper (TM), and Enhanced Thematic Mapper Plus (ETM+) data with reflective wavelength pixel sizes of 80, 30, and 30 m, respectively, are resampled to 60 m and then classified by visual interpretation, inspection of aerial photography, and ground survey, into 10 classes (Table 1, first column). The classes are defined to capture LCLU discernable in the Landsat data and include mechanically disturbed (forest clear cutting, earthmoving, or reservoir draw down) and naturally disturbed classes (due to wind, fire, or insect infestation) that describe land that is in an altered unvegetated state. The Landsat data are located using a stratified random sampling methodology with respect to the 84 contiguous level III ecoregions defined by *Omernik* [1987]. At the time of writing only 58 of the 84 ecoregions have been processed by the United States Geological Survey and these are used in this study.

[6] Figure 1 shows the CONUS study area and the 58 ecoregions that have Landsat-derived LCLU data generated to date. The ecoregion numbering system (1–84) used to refer to specific ecoregions is illustrated in Figure 1. In each ecoregion, classification of 10 × 10 km or 20 × 20 km Landsat spatial subsets acquired in 1973, 1980, 1986, 1992, and 2000 was performed. A total of 1796 subsets fall in the 58 ecoregions and are located using a stratified random sampling methodology with 9–48 Landsat classified spatial subsets per ecoregion. The sampling was designed to enable a statistically robust "scaling up" of the classification data to estimate areal LCLU class proportions and LCLU class temporal change within each ecoregion [*Stehman et al.*, 2005]. The 58 ecoregions cover 69% of the CONUS and vary in area from 14,458 km^2 (Willamette Valley, ecoregion 3) to 346,883 km^2 (Northwestern Great Plains, ecoregion 43). Statistical estimates of the LCLU class proportions in each of these ecoregions [*Stehman et al.*, 2005] and the classified Landsat subsets that fall within them for years 1973 and 2000 are used in this study.

[7] Albedo data are provided by the most recent MODIS Collection 5 bidirectional reflectance distribution function (BRDF)/Albedo 16 day 500 m product [*Schaaf et al.*, 2002]. The MODIS BRDF/Albedo product is generated every 8 days by inversion of the Ross-Thick/Li sparse reciprocal bidirectional reflectance distribution function (BRDF) model against the MODIS observations (surface reflectance and solar and viewing geometry values) sensed in a 16 day period [*Schaaf et al.*, 2002, 2008]. The MODIS albedo product provides both the black-sky albedo (directional-hemispherical reflectance) computed by integration of the BRDF over all view angles, and the white-sky albedo (bihemispherical reflectance under isotropic illumination) derived by a further integration over all solar zenith angles [*Schaaf et al.*, 2002]. In this work the MODIS broadband (0.3–5.0 μm) white-sky albedo and associated per-pixel product quality assessment information that describe the processing method and whether a snow or snow-free albedo was retrieved are used. Only good quality (full BRDF inversion), nonfill, snow, and snow-free albedo values are used. Nine years of MODIS 500 m broadband white-sky albedo, 18 February 2000 to 31 March 2009, defined every 8 days are used in order to capture interannual albedo variability.

[8] Snow cover data are provided by the MODIS Collection 5 monthly average snow cover 0.05° climate modeling grid product (MOD10CM) [*Hall et al.*, 2006; *Hall and Riggs*, 2007]. The monthly products for January 2004 to December 2008 (the complete full years currently available) are used to compute ecoregion monthly snow climatology, i.e., the mean fractional snow cover (0–1) for each calendar month, and the mean of the 12 monthly values are used to compute the ecoregion mean annual snow fraction.

[9] Monthly incoming surface solar radiation downward (SSRD) are provided in 2.5° × 2.5° cells from January 1973 to December 2000 by the European Center for Medium Range Weather Forecasts 40 year Reanalysis (ERA-40) data set [*Allan et al.*, 2004]. ERA-40 is a 45-year second-generation reanalysis that has been reprocessed with more observations and makes more comprehensive use of satellite data re-processed from raw observations where possible [*Uppala et al.*, 2005]. These data are used to define mean monthly SSRD climatology in watts per meter square (Wm^{-2}) for each ecoregion.

3. Methods

3.1. Ecoregion LCLU Class Monthly Albedo

[10] MODIS 500 m broadband white-sky albedo values were extracted at fixed geographic locations defined by analysis of the 60 m Landsat 2000 LCLU classified subsets. In each of the 58 ecoregions, there were 9–48 Landsat 2000

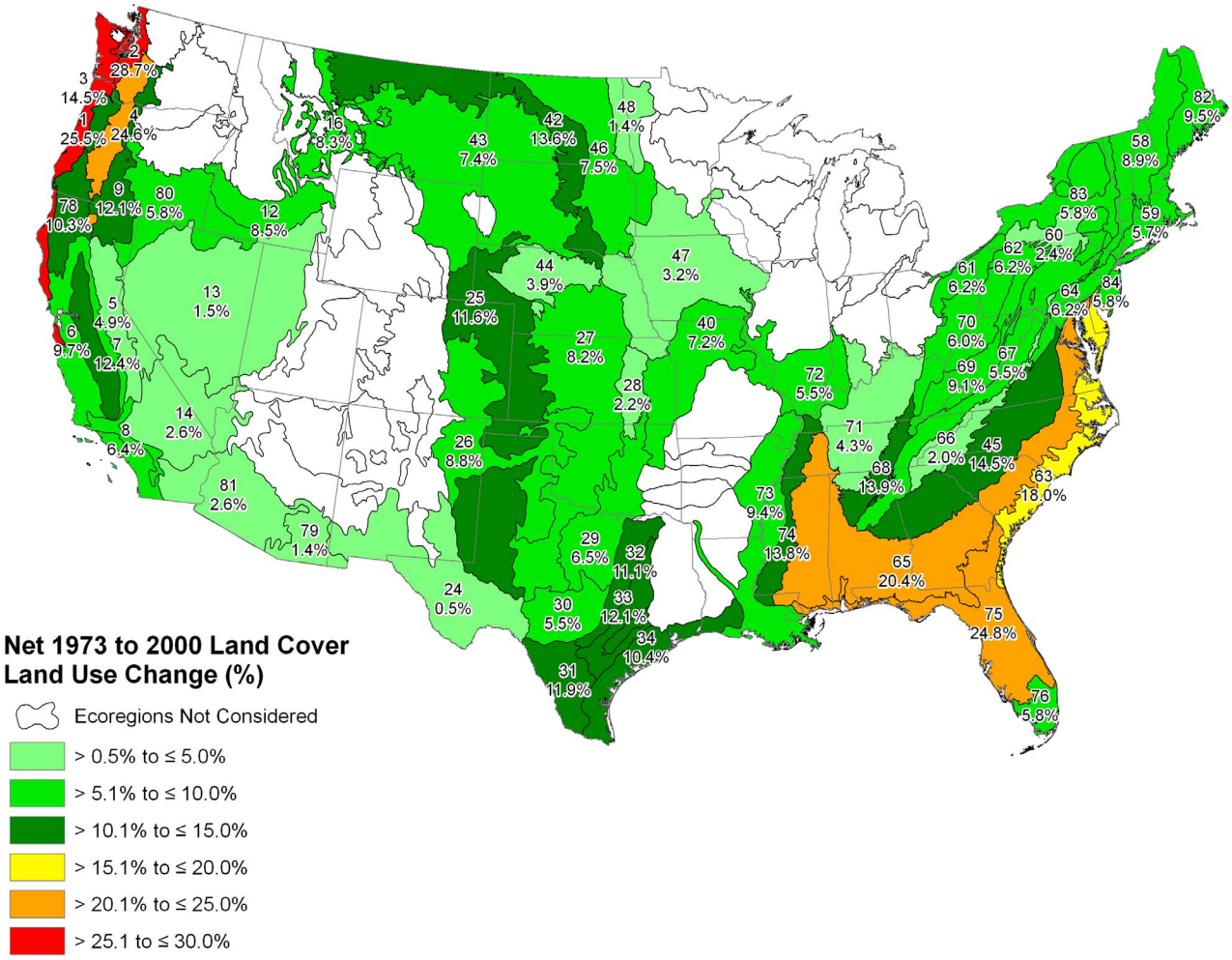

Figure 1. Completed ecoregions to date (colored and numbered) and their percentage of land cover land use changes from 1973 to 2000.

LCLU classified subsets; in the larger ecoregions, there were more Landsat subsets, and so typically more albedo values available for extraction. To ensure that the MODIS 500 m pixels contained only a single LCLU class, the boundaries of each LCLU class in each subset were morphologically eroded by 240 m [*Serra*, 1982]. MODIS albedo values were then extracted at the remaining LCLU class centroids from the 9 year time series of MODIS albedo data starting after each Landsat subset 2000 acquisition date to 31 March 2009. A total of 60,423 snow and 1,307,902 snow-free MODIS albedo values were extracted.

[11] The median snow and snow-free monthly albedo was computed from the 9 years of MODIS data for each LCLU class, ecoregion, and month as

$$\overline{\alpha}_{i,\ \text{ecoregion},\ \text{month},\ \text{snow}} = \underset{9\ \text{years}}{\text{median}}\left\{\text{snow albedo}_{i,\ \text{ecoregion},\ \text{month}}\right\}$$

$$\overline{\alpha}_{i,\ \text{ecoregion},\ \text{month},\ \text{snow-free}} = \underset{9\ \text{years}}{\text{median}} \cdot \left\{\text{snow-free albedo}_{i,\ \text{ecoregion},\ \text{month}}\right\}, \quad (1)$$

where $\overline{\alpha}_{i,\ \text{ecoregion},\ \text{month},\ \text{snow}}$ and $\overline{\alpha}_{i,\ \text{ecoregion},\ \text{month},\ \text{snow-free}}$ are the monthly median snow and snow-free monthly albedos for LCLU class *i*, respectively, in the ecoregion, and snow albedo and snow-free albedo are the snow and snow-free broadband white-sky MODIS 500 m albedo values. The median rather than the mean value was taken as it is less sensitive to infrequent but anomalously low or high MODIS albedo values associated with residual shadow or cloud contamination [*Román et al.*, 2009].

[12] In some ecoregions, and for certain months and LCLU classes, there were insufficient MODIS snow and snow-free albedos to estimate (1). This typically occurred in ecoregions with small areal LCLU class proportions (<0.005), in persistently cloudy months, and for the snow albedo in snow-free ecoregions and summer months. In these cases the median monthly (snow or snow-free) class albedos computed for each ecoregion with at least 3 valid (nonfill, full BRDF inversion) class albedo values were

computed, and the median of the CONUS median albedo values used as

$$\overline{\alpha}_{i,\ \text{ecoregion},\ \text{month},\ \text{snow}} = \underset{58\ \text{ecoregions}}{\text{median}} \cdot \left\{ \underset{9\ \text{years}}{\text{median}} \left\{ \text{snow albedo}_{i,\ \text{ecoregion},\ \text{month}} \right\} \right\}$$
$$\overline{\alpha}_{i,\ \text{ecoregion},\ \text{month},\ \text{snow-free}} = \underset{58\ \text{ecoregions}}{\text{median}} \cdot \left\{ \underset{9\ \text{years}}{\text{median}} \left\{ \text{snow-free albedo}_{i,\ \text{ecoregion},\ \text{month}} \right\} \right\}, \quad (2)$$

where $\overline{\alpha}_{i,\ \text{ecoregion},\ \text{month},\ \text{snow}}$ and $\overline{\alpha}_{i,\ \text{ecoregion},\ \text{month},\ \text{snow-free}}$ are the monthly median snow and snow-free monthly albedos for LCLU class i, respectively.

[13] The median albedos were used to estimate the ecoregion monthly LCLU class albedos, following the approach of *Roesch et al.* [2002], as

$$\alpha_{i,\ \text{ecoregion},\ \text{month}} = \left(1 - f_{\text{snow},\ \text{month},\ \text{ecoregion}}\right) \overline{\alpha}_{i,\ \text{ecoregion},\ \text{month},\ \text{snow-free}} + f_{\text{snow},\ \text{month},\ \text{ecoregion}} \overline{\alpha}_{i,\ \text{ecoregion},\ \text{month},\ \text{snow}}, \quad (3)$$

where $\alpha_{i,\ \text{ecoregion},\ \text{month}}$ is the monthly albedo for LCLU class i and $\overline{\alpha}_{i,\ \text{ecoregion},\ \text{month},\ \text{snow}}$ and $\overline{\alpha}_{i,\ \text{ecoregion},\ \text{month},\ \text{snow-free}}$ are the median snow and snow-free monthly albedos for LCLU class i, respectively, defined as equation (1) or (2), and $f_{\text{snow},\ \text{month},\ \text{ecoregion}}$ is the monthly snow fraction [0–1] derived from the MODIS snow product.

3.2. Ecoregion Monthly Albedo

[14] An estimate of the monthly albedo for each ecoregion and year was computed independently for the LCLU class areal proportions in 1973 and 2000 as

$$\alpha_{\text{ecoregion},\ \text{month},\ \text{year}} = \sum_{i=1}^{10} \left(p_{i,\ \text{ecoregion},\ \text{year}} \alpha_{i,\ \text{ecoregion},\ \text{month}} \right), \quad (4)$$

where year is 1973 or 2000, and for each LCLU class i, p_i is the LCLU class areal proportion in the ecoregion for the year defined by the USGS Land Cover Trends Project data [*Stehman et al.*, 2005], and $\alpha_{i,\ \text{ecoregion},\ \text{month}}$ is defined as equation (3).

[15] To help interpret our results, the annual LCLU-induced albedo change from 1973 to 2000 was computed as

$$\Delta\alpha_{\text{ecoregion},\ \text{annual}} = \frac{\sum_{\text{month}=1}^{12} \left(\alpha_{\text{ecoregion},\ \text{month},\ 2000} - \alpha_{\text{ecoregion},\ \text{month},\ 1973} \right)}{12}, \quad (5)$$

where $\alpha_{\text{ecoregion},\ \text{month},\ \text{year}}$ is defined as equation (4).

3.3. Ecoregion Monthly Albedo Interannual Variability

[16] The interannual monthly albedo variability was estimated for each LCLU class as

$$\text{MAD}_{i,\ \text{ecoregion},\ \text{month}} = \underset{9\ \text{years}}{\text{median}} \cdot \left\{ \left| \overline{\alpha}_{i,\ \text{ecoregion},\ \text{month},\ \text{snow-free}}, - \underset{9\ \text{years}}{\text{median}} \cdot \left\{ \overline{\alpha}_{i,\ \text{ecoregion},\ \text{month},\ \text{snow-free}} \right\} \right| \right\}, \quad (6)$$

where $\text{MAD}_{i,\ \text{ecoregion},\ \text{month}}$ is the albedo median absolute deviation (MAD) for each LCLU class i, month, and ecoregion, and $\overline{\alpha}_{i,\ \text{ecoregion},\ \text{month},\ \text{snow-free}}$ is defined as equation (1) or (2). These MAD values reflect for each month the interannual albedo variation derived over the 9 years of MODIS data from 2000 to 2009. The MAD rather than the standard deviation was used as it is less sensitive to infrequent but anomalously low or high MODIS albedo values. Only snow-free MODIS albedo data were considered as many ecoregions had insufficient snow albedo LCLU class values in each month to compute MAD statistics. Interannual albedo variability statistics were computed for snow-free conditions for a total of 45 ecoregions.

[17] The inter-annual monthly albedo variability for each ecoregion was estimated as

$$\text{MAD}_{\text{ecoregion},\ \text{month},\ \text{year}} = \sum_{i=1}^{10} \left(p_{i,\ \text{ecoregion},\ \text{year}} \text{MAD}_{i,\ \text{ecoregion},\ \text{month}} \right), \quad (7)$$

where for each LCLU class i, p_i is the LCLU class areal proportion in the ecoregion defined for year 1973 or 2000, $\alpha_{i,\ \text{ecoregion},\ \text{month}}$ is defined as equation (3) and $MAD_{i,\ \text{ecoregion},\ \text{month}}$ is defined as equation (6).

[18] To help interpret our results, the percentage average monthly variation in the ecoregion albedo due to interannual albedo variability was computed as

$$\nu_{\text{ecoregion},\ \text{year}} = \frac{\sum_{\text{month}=1}^{12} \left(\text{MAD}_{\text{ecoregion},\ \text{month},\ \text{year}} \Big/ \alpha_{\text{ecoregion},\ \text{month},\ \text{year}} \right)}{12} \times 100, \quad (8)$$

where *year* is 1973 or 2000 and $\text{MAD}_{\text{ecoregion},\ \text{month},\ \text{year}}$ is defined as equation (7) and $\alpha_{\text{ecoregion},\ \text{month},\ \text{year}}$ is defined as equation (4).

3.4. Surface Radiative Forcing Due to LCLU Albedo Change From 1973 to 2000

[19] In each ecoregion, the monthly surface radiative forcing (Wm^{-2}) due to LCLU albedo change from 1973 to 2000 was estimated following [*Jin and Roy*, 2005; *Barnes and Roy*, 2008] as

$$\Delta F_{\text{ecoregion},\ \text{month}} = \overline{I}^{\downarrow}_{\text{ecoregion},\ \text{month}} \cdot \left(\alpha_{\text{ecoregion},\ \text{month},\ 2000} - \alpha_{\text{ecoregion},\ \text{month},\ 1973} \right), \quad (9)$$

where $-\overline{I}^{\downarrow}_{\text{ecoregion},\ \text{month}}$ is the mean monthly incoming SSRD climatology (Wm^{-2}) for the ecoregion, and $\alpha_{\text{ecoregion},\ \text{month},\ 2000}$ and $\alpha_{\text{ecoregion},\ \text{month},\ 1973}$ are the monthly ecoregion albedos for 2000 and 1973, respectively, defined as equation (4). The annual surface radiative forcing (Wm^{-2}) in each ecoregion due to LCLU albedo change from 1973 to 2000 was computed as

$$\Delta F_{\text{ecoregion},\ \text{annual}} = \frac{\sum_{\text{month}=1}^{12} \Delta F_{\text{ecoregion},\ \text{month}}}{12}, \quad (10)$$

where $\Delta F_{\text{ecoregion},\ \text{month}}$ is defined by equation (9).

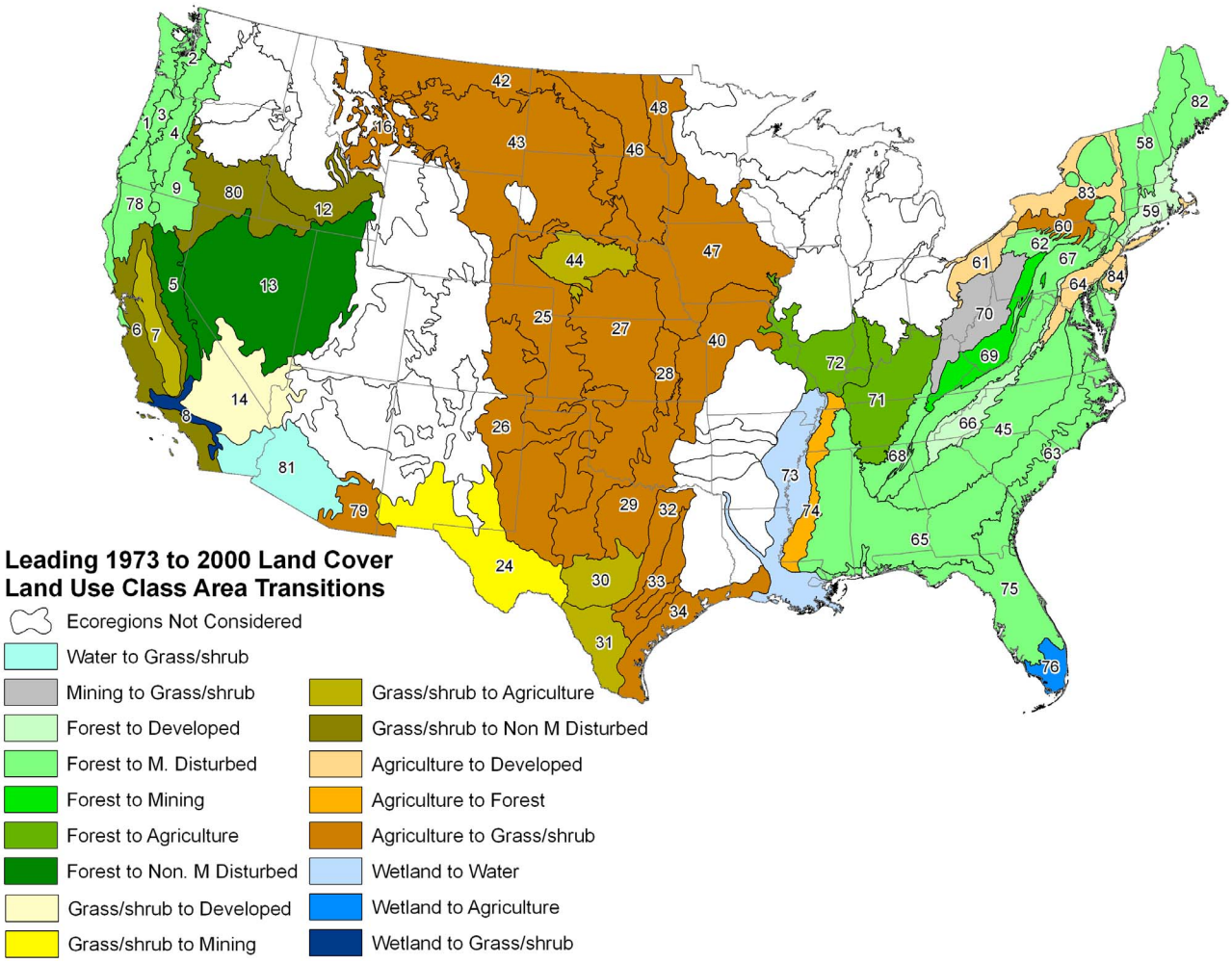

Figure 2. Leading 1973–2000 class transitions by areal change for the 58 ecoregions considered in this study (numbered).

[20] The CONUS scale net surface radiative forcing (Wm^{-2}) was estimated as

$$\Delta F_{\mathrm{CONUS,\ annual}} = \frac{\sum_{\mathrm{ecoregion}\,=\,1}^{58} a_{\mathrm{ecoregion}}\ \Delta F_{\mathrm{ecoregion,\ annual}}}{\sum_{\mathrm{ecoregion}\,=\,1}^{58} a_{\mathrm{ecoregion}}}, \quad (11)$$

where $\alpha_{\mathrm{ecoregion}}$ is the ecoregion area (km^2) and $\Delta F_{\mathrm{ecoregion,\ annual}}$ is defined by equation (10).

3.5. Sensitivity of Surface Radiative Forcing Due to Interannual Albedo Variability

[21] The sensitivity of the monthly surface radiative forcing was estimated by applying standard propagation of variance formulae to equation (9), assuming that there was no error in the incoming SSRD climatology (as this is not defined) and that the monthly ecoregion albedos for 2000 and 1973 were independent, as

$$\varepsilon_{\Delta F_{\mathrm{ecoregion,\ month}}} = -\bar{I}^{\downarrow}_{\mathrm{ecoregion,\ month}} \sqrt{\varepsilon^2_{\alpha_{\mathrm{ecoregion,\ month,\ 2000}}} + \varepsilon^2_{\alpha_{\mathrm{ecoregion,\ month,\ 1973}}}}, \quad (12)$$

where $\varepsilon_{\Delta F_{\mathrm{ecoregion,\ month}}}$ is the monthly ecoregion surface radiative forcing error, $-\bar{I}^{\downarrow}_{\mathrm{ecoregion,\ month}}$ is the mean monthly incoming SSRD climatology (Wm^{-2}) for the ecoregion, and $\varepsilon_{\alpha_{\mathrm{ecoregion,\ month,\ 2000}}}$ and $\varepsilon_{\alpha_{\mathrm{ecoregion,\ month,\ 1973}}}$ are defined as

$$\varepsilon_{\alpha_{\mathrm{ecoregion,month,year}}} = \left(\sum_{i=1}^{10} \left(p_{i,\mathrm{ecoregion,year}} \mathrm{MAD}_{i,\,\mathrm{ecoregion,month}} \right) \right), \quad (13)$$

where, for each LCLU class i, p_i is the class areal proportion in the ecoregion for the year defined by the USGS Land Cover Trends Project data [*Stehman et al.*, 2005] and $\mathrm{MAD}_{i,\ \mathrm{ecoregion,\ month}}$ is the albedo median absolute deviation defined by equation (6).

[22] The sensitivity of the annual surface radiative forcing imposed by interannual albedo variability was estimated by applying standard propagation of variance formulae to equation (10), assuming that the monthly forcing estimates were independent as

$$\varepsilon_{\Delta F_{\mathrm{ecoregion,\ annual}}} = \frac{1}{12} \sqrt{\sum_{\mathrm{month}\,=\,1}^{12} \varepsilon^2_{\Delta F_{\mathrm{ecoregion,\ month}}}} \quad (14)$$

where $\varepsilon_{\Delta F_{\mathrm{ecoregion,\ month}}}$ is defined by equation (12).

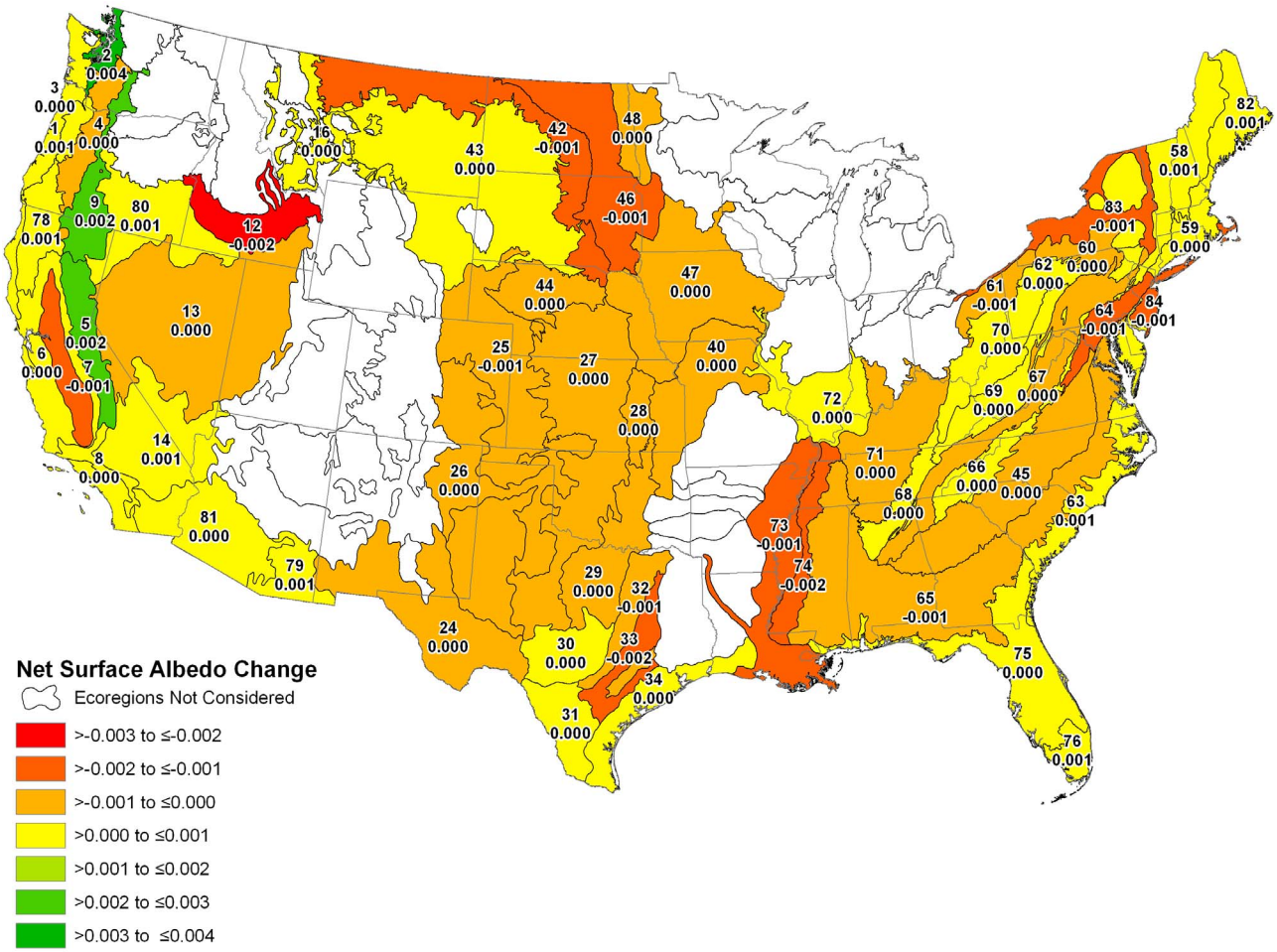

Figure 3. The annual surface albedo change due to contemporary land cover land use change from 1973 to 2000 modeling snow conditions, for the 58 ecoregions considered in this study.

[23] Similarly, the CONUS scale net surface radiative forcing error was estimated by applying standard propagation of variance formulae to equation (11), assuming that the ecoregion area estimates were without error and that the monthly forcing estimates were independent as

$$\varepsilon_{\Delta F_{\mathrm{CONUS,\ annual}}} = \sqrt{\sum_{\mathrm{ecoregion}=1}^{n} \left(\left(\frac{a_{\mathrm{ecoregion}}}{\sum_{1}^{n} a_{\mathrm{ecoregion}}} \right)^2 \varepsilon^2_{\Delta F_{\mathrm{ecoregion,\ annual}}} \right)}, \tag{15}$$

where $\alpha_{\mathrm{ecoregion}}$ is the ecoregion area (km^2) and $\varepsilon_{\Delta F_{\mathrm{ecoregion,\ annual}}}$ is defined by equation (14) and n is the number of ecoregions considered.

4. Results

4.1. LCLU Change From 1973 to 2000

[24] Between 1973 and 2000 all of the 58 ecoregions considered had LCLU change (Figure 1). The greatest estimated percentage areal changes occurred in the northwest: 28.7% in the Puget Lowland (ecoregion 2), 25.5% Coast Range (ecoregion 1), and 14.5% Willamette Valley (ecoregion 3), and in the southeast: 24.8% in the Southern Coastal Plain (ecoregion 75) and 20.4% in the Southeastern Plains (ecoregion 65). The smallest estimated percentage areal changes occurred in the Chihuahuan Desert (ecoregion 24), 0.5%, and in the Lake Agassiz Plain (ecoregion 48), 1.4%. At the CONUS scale, the dominant LCLU changes were a net areal decrease in agricultural land from 1.652 million km^2 in 1973 to 1.577 million km^2 in 2000 and a net areal increase in developed land from 194.3 thousand km^2 in 1973 to 259.0 thousand km^2 in 2000.

[25] Figure 2 illustrates the leading LCLU class transitions by areal change from 1973 to 2000 for the ecoregions considered. The greatest amounts of change were generally in ecoregions with active timber harvesting, whereas the lowest amounts of change were in ecoregions where urbanization was the leading change. A transition of agriculture to grass/shrub was concentrated in the Great Plains ecoregions and can be attributed primarily to the 1985 Farm Bill that established the Conservation Reserve Program [*Johnson and Maxwell*, 2001]. This voluntary program offered financial incentives for farmers to retire marginal agricultural land to native grasses or trees, usually for 10 years in duration. A transition from forest to mechanically

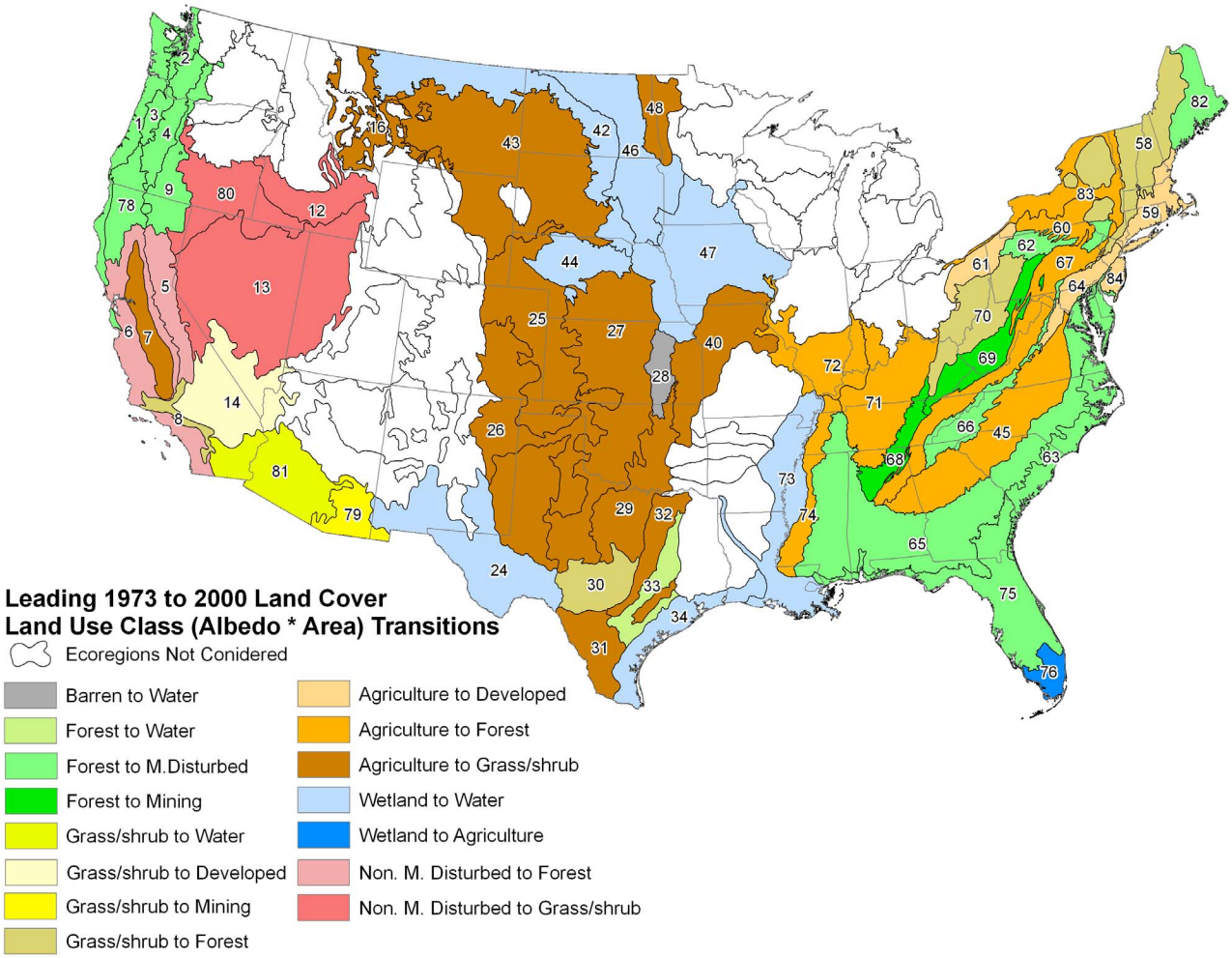

Figure 4. Leading land cover land use class transitions due to albedo and areal land cover land use change from 1973 to 2000 modeling snow conditions, for the 58 ecoregions considered in this study.

disturbed classes occurred primarily in ecoregions of the Pacific Northwest and in the East, which is indicative of the active timber harvesting industries in these ecoregions. All ecoregions experienced significant increases in developed land between 1973 and 2000 [*Loveland and Acevedo*, 2010] but were not the leading LCLU class area transition. The pattern of LCLU change is driven primarily by agricultural abandonment, by ex-urban development, and by government policy [*Loveland and Acevedo*, 2010]. The purpose of this paper is to quantify the surface albedo radiative forcing impact of these LCLU changes and so the driving forces of LCLU changes are not discussed further.

4.2. CONUS MODIS Albedo Estimates

[26] Table 1 summarizes the MODIS broadband white-sky snow and snow-free albedos for the 10 LCLU classes derived from all of the valid CONUS MODIS albedo data. These values are included to help interpret the LCLU class albedos only, they are not used in the forcing analysis.

[27] The snow-free albedo class values summarized in Table 1 are comparable to those described by *Jin et al.* [2002] and *Zou et al.* [2003], and the snow albedos are comparable to those of *Gao et al.* [2005] and *Myhre and Myhre* [2003]. Snow increases least the albedo of the vegetated surfaces with high canopy density and vertical structure (e.g., evergreen forests) and increases most the albedo of surfaces with sparse and/or short vegetation (e.g., barren). The barren and agricultural classes have the highest snow and snow-free albedos, and the water and forest classes have the lowest albedos. The forest class, which includes deciduous and coniferous types, has the smallest difference between snow and snow-free albedo of 0.243 and 0.130, respectively, which is due mainly to snow being hidden underneath the forest. *Betts and Ball* [1997] found similar snow to snow-free albedo differences for boreal forest albedo that they noted seldom exceeds 0.3.

4.3. LCLU Albedo Change From 1973 to 2000

[28] The ecoregion annual LCLU induced albedo change from 1973 to 2000 computed as equation (5) is illustrated in Figure 3. *Barnes and Roy* [2008] demonstrated that albedo change associated with LCLU change is dependent on the albedo of the LCLU classes and on the areal extent of the LCLU change. Hence, the ecoregions with the highest areal proportions of LCLU change (Figure 1) do not consistently coincide with the ecoregions of highest albedo change

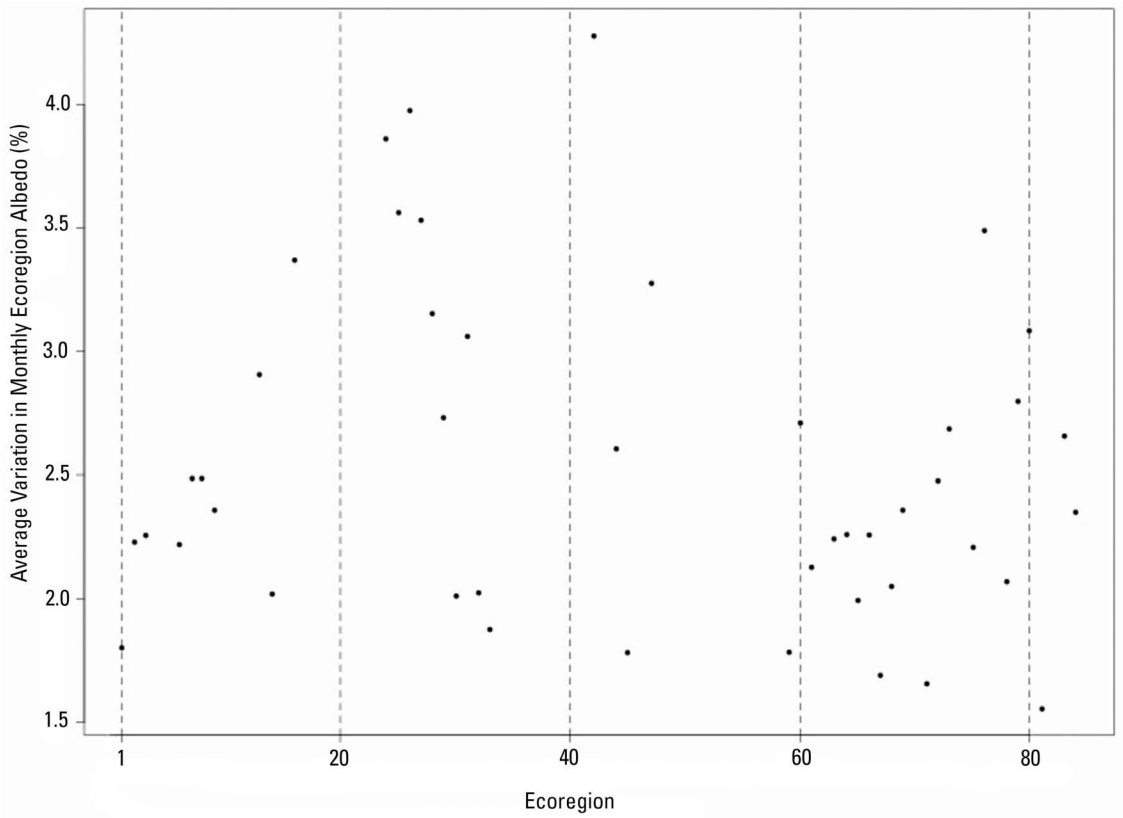

Figure 5. Ecoregion percent average monthly variation in ecoregion albedo due to interannual albedo variability, defined as equation (8), for the year 2000 LCLU class proportions. Only snow-free results for 45 ecoregions where interannual variability statistics can be computed are illustrated.

(Figure 3), and the correlation between these data is low (0.192).

[29] Figure 4 illustrates the leading LCLU class transitions that resulted in the greatest absolute change in albedo from 1973 to 2000. The leading LCLU class transitions shown in Figure 4 do not always coincide with the leading transitions due only to LCLU areal change shown in Figure 2. LCLU change between classes with different albedos may have a greater net albedo impact than more areally extensive changes between classes with similar albedos. For example, in the Eastern Great Lakes and Hudson Lowlands (ecoregion 83, mean annual snow fraction 0.18), the primary areal LCLU transition is from agriculture to developed (Figure 2), whereas the primary (areal and albedo) transition is from agriculture to forest (Figure 4). More than half of the ecoregions in this study had a different leading LCLU transition when areal and albedo were considered compared to considering LCLU areal change only.

[30] Figure 5 illustrates, for the 2000 LCLU class proportions, the 12 month average monthly variation in ecoregion albedo due to interannual variability equation (8). Only results for 45 of the 58 ecoregions that had sufficient snow-free MODIS albedo data to compute the MAD statistics that capture interannual albedo variability are shown. The results for 1973 are not plotted and are very similar to the 2000 results (0.999 correlation over the 45 ecoregions). The minimum, median, and maximum interannual albedo variability percentages were 1.6%, 2.4%, and 4.3%, respectively. The maximum occurred in the Northwestern Glaciated Plains (ecoregion 42) that was primarily agriculture (57%) and grass/shrub (37%). The other two maxima occurred in ecoregions 26 (Southwestern Tablelands, interannual albedo variability, 4.0%) and 24 (Chihuahuan Deserts, interannual albedo variability, 3.9%) that in 2000 both had a primary LCLU class proportion of grass/shrub (82% and 96%, respectively).

4.4. Surface Radiative Forcing Due to LCLU Albedo Change From 1973 to 2000

[31] Figure 6 illustrates the annual surface radiative forcing due to contemporary LCLU albedo change from 1973 to 2000, for the 58 ecoregions considered in this study, estimated using equation (10) by taking into consideration the monthly variation of albedo, snow cover, and incoming SSRD. The geographic distribution of the annual surface radiative forcing is strongly correlated (−0.956) with the annual 1973–2000 LCLU albedo change (Figure 3) and only weakly (−0.068) with the annual incoming SSRD.

[32] The geographic distribution of surface radiative forcing cooling or warming illustrated in Figure 6 is complex. The most negative surface radiative forcing, i.e., cooling, was -0.367 Wm^{-2} and occurred in the Sierra Nevada (ecoregion 5) due primarily to the transition of nonmechanically disturbed to forest (Figure 4). The most

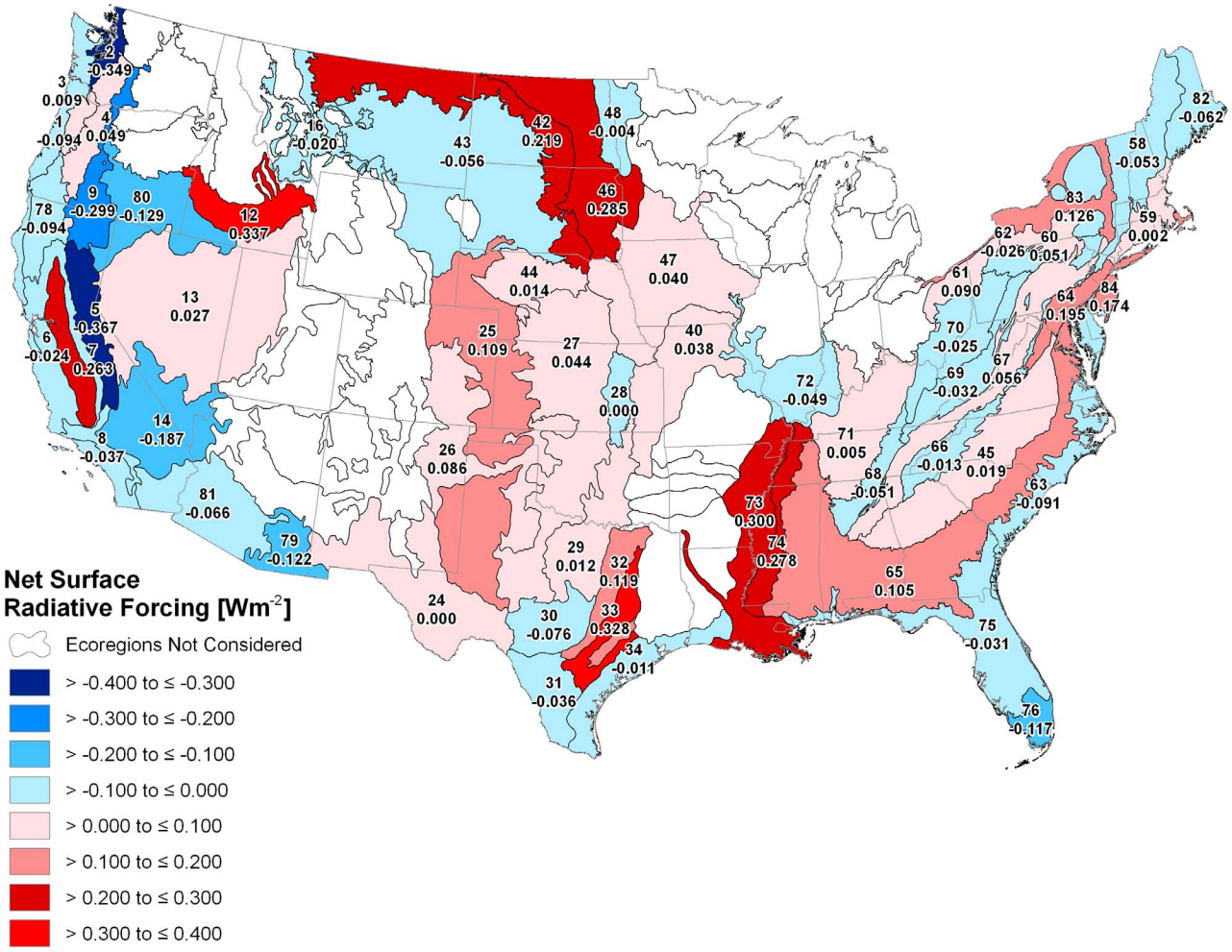

Figure 6. The annual surface radiative forcing due to contemporary land cover land use albedo change from 1973 to 2000 modeling snow conditions, for the 58 ecoregions considered in this study.

positive forcing, i.e., warming, was 0.337 Wm^{-2} in the Snake River Basin (ecoregion 12) due primarily to the conversion of nonmechanically disturbed to grass/shrub. This magnitude of ecoregion forcing is not insignificant, for example, it is greater than the magnitude of global forcing estimates due to LCLU change since 1750 [*IPCC*, 2007].

[33] At the CONUS scale, we estimate a positive (i.e., warming) net surface radiative forcing of 0.029 Wm^{-2} due to LCLU albedo change from 1973 to 2000 equation (11). This CONUS net surface radiative forcing is greater than our earlier reported result of 0.012 Wm^{-2} [*Barnes and Roy*, 2008], which we attribute to considering 26% more area of the CONUS in this study and because we modeled snow effects that we demonstrate below is important for certain LCLU transitions and ecoregions.

4.5. Snow Sensitivity Analysis of Surface Radiative Forcing Due to LCLU Albedo Change From 1973 to 2000

[34] The impact of snow has been shown to be important when LCLU change is between snow-hiding and snow-revealing classes, such as between forest and grass/shrub or agricultural classes [*Betts*, 2000; *Gao et al.*, 2005; *Gibbard et al.*, 2005; *Wang and Davidson*, 2007]. The mean annual snow fraction for years 2004–2008 derived from the MODIS global monthly average snow product is illustrated in Figure 7. Of the 58 ecoregions considered, 22 had more than 0.10 mean annual snow fraction. The greatest mean annual snow fraction occurred predominantly in the northern ecoregions, up to 0.30 in the Laurentian Plains and Hills (ecoregion 82) but also in some high-altitude ecoregions such as the Cascades (0.27) (ecoregion 4). The southernmost ecoregions had mean annual snow fraction <0.10.

[35] A scatterplot of the annual surface radiative forcing due to LCLU albedo change, modeling snow and snow-free conditions, for the 58 ecoregions is illustrated in Figure 8. The surface radiative forcing modeling snow-free conditions was computed by setting the monthly snow fraction ($f_{snow,\ month,\ ecoregion}$) in equation (3) to zero. The illustrated sensitivity is determined by the extent of the LCLU change, the snow and snow-free albedos of the LCLU change classes, and the monthly snow fraction. Consequently, ecoregions with low snow fraction had little or no radiative forcing sensitivity (southern ecoregions), and ecoregions with high

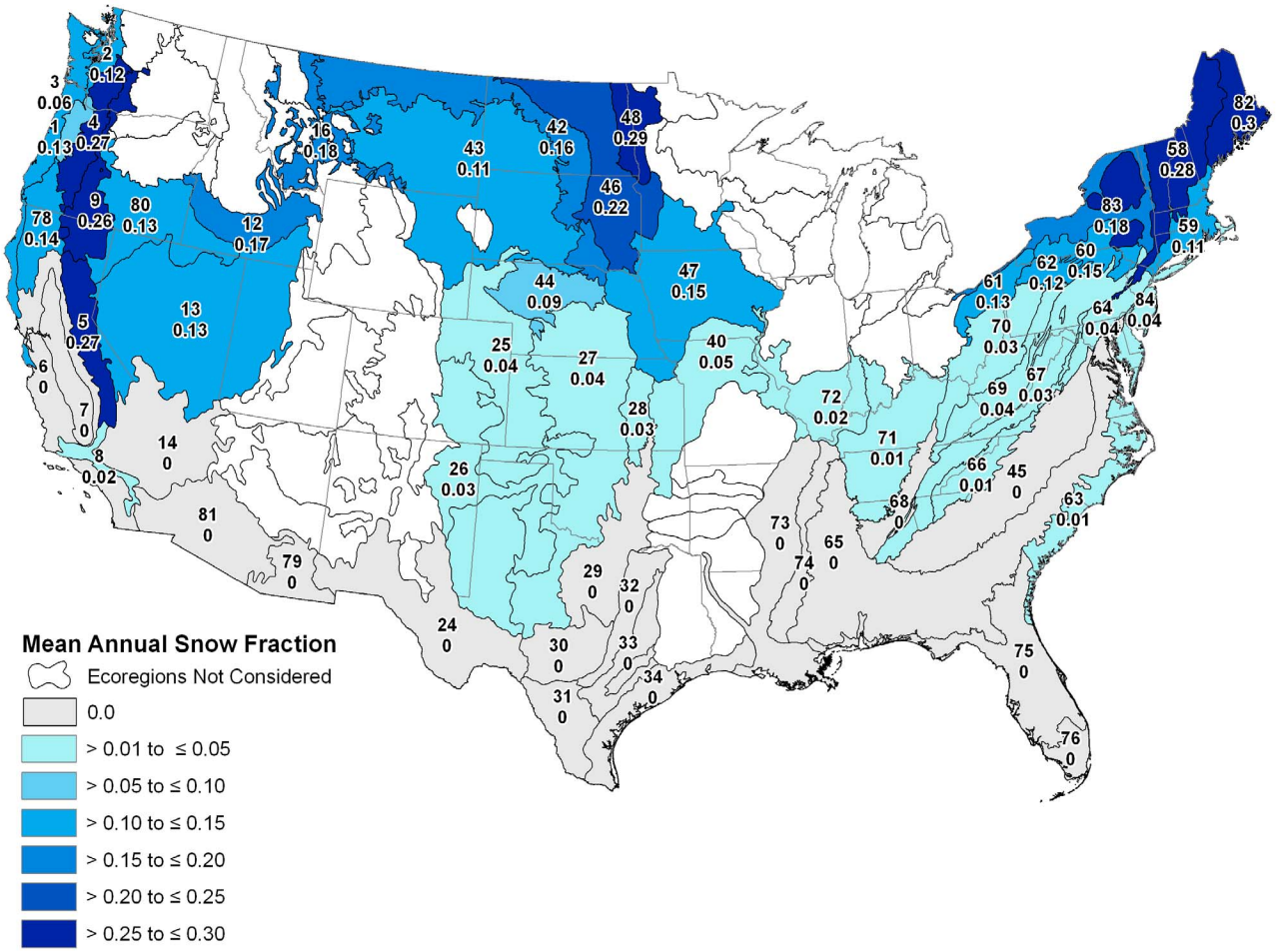

Figure 7. The mean annual snow fraction from years 2004 to 2008 derived from the MODIS 0.05° cell global monthly average snow cover product [*Hall et al.*, 2006], for the 58 ecoregions considered in this study (numbered), and their snow fraction.

snow fraction had a greater radiative forcing sensitivity (predominantly northern ecoregions). The annual snow fraction values for ecoregions with snow fractions >0.10 are labeled in Figure 8 for visual reference.

[36] Ecoregions 42 (Northwestern Glaciated Plains) and 46 (Northern Glaciated Plains) had high annual snow fractions of 0.16 and 0.22, respectively, but had a negligible radiative forcing sensitivity to snow albedo effects (Figure 8, points lying close to the 1:1 line, top right). This is because in both these ecoregions the primary LCLU transition was from agriculture to grass/shrub (Figure 2), i.e., transitions between snow revealing LCLU classes with similar albedos.

[37] In snow-prone ecoregions where LCLU transitions were between snow-hiding and snow-revealing LCLU classes, the surface radiative forcing becomes more negative or more positive when snow is modeled (Figure 8). The most extreme example of this effect is ecoregion 5 (Sierra Nevada, 0.27 annual snow fraction) that had a surface radiative forcing of -0.367 Wm^{-2} (modeling snow conditions) and -0.160 Wm^{-2} (modeling snow-free conditions). Figure 9 shows the monthly surface radiative forcing, albedo change, SSRD, and snow fraction values for ecoregion 5. The seasonal variation of these values is very evident. During the winter months (December, January, February, March), the monthly snow fraction is between 0.57 and 0.73. When snow is modeled (black circles), the winter monthly albedo change and surface radiative forcing estimates are significantly higher and lower, respectively, than the snow-free (white circles) estimates. This is because for this ecoregion, the primary LCLU transition is from forest to nonmechanically disturbed, i.e., snow-hiding to snow-revealing classes.

[38] At the CONUS level, failure to model snow albedo conditions results in an overestimation in the net CONUS surface radiative forcing. We estimated a net CONUS surface radiative forcing of 0.029 Wm^{-2} due to LCLU albedo change from 1973 to 2000 when snow is modeled (section 4.4) and 0.031 Wm^{-2} when snow is not modeled.

4.6. Radiative Forcing Sensitivity Analysis to Interannual Variability

[39] Figure 10 illustrates the annual surface radiative forcing due to contemporary LCLU albedo change for each ecoregion (black circles) and the associated forcing error (vertical error bar lines) defined by equations (10) and (14), respectively. These values are based on median and MAD

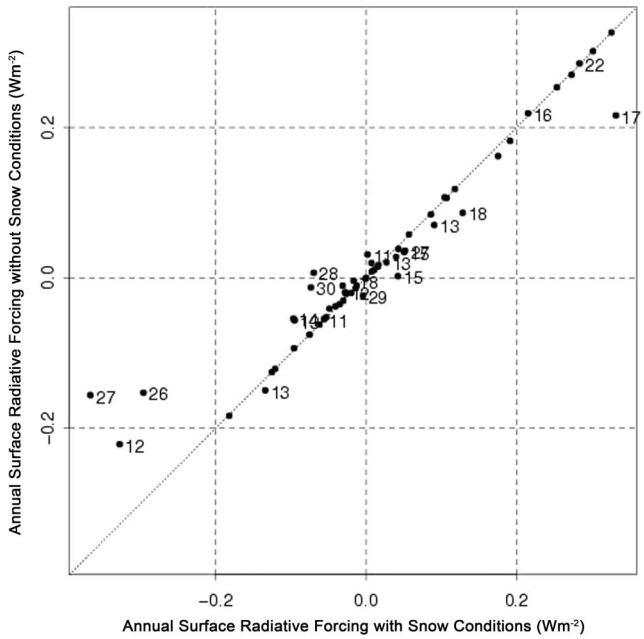

Figure 8. Scatterplot of the annual surface radiative forcing modeling snow (*x* axis) and snow-free (*y* axis) effects, for the 58 ecoregions considered in this study (black dots); some ecoregions have similar values and so overlap. The mean seasonal snow fraction values for ecoregions with snow fractions >0.10 are labeled (values are shown multiplied by 100 for visual clarity).

albedo estimates, respectively; the errors are expected to describe 50% of the surface radiative forcing variability around the annual estimates. Only snow-free forcing results for 45 of the 58 ecoregions considered in this study are illustrated.

[40] The annual surface radiative forcing error estimates are a function of the magnitude of the incoming SSRD and the interannual monthly class albedo variability equation (14). The errors are correlated with the incoming SSRD (0.591) and with the estimates of the 12 month average monthly variation in ecoregion albedo due to interannual variability (0.753 for both $v_{\text{ecoregion, 1973}}$ and $v_{\text{ecoregion, 2000}}$). The minimum error (0.138 Wm^{-2}) occurred in the Northeastern Coastal Zone (ecoregion 59) because of a combination of relatively low incoming SSRD found at higher latitudes (ecoregion 59 has a 168.2 Wm^{-2} mean annual SSRD) and low interannual monthly class albedo variability (1.8% for $v_{\text{ecoregion, 1973}}$ and $v_{\text{ecoregion, 2000}}$). The maximum annual surface radiative forcing error (0.842 Wm^{-2}) occurred in the Chihuahuan Deserts (ecoregion 24) and was driven by the high incoming SSRD (this ecoregion has the fifth highest mean annual SSRD of 237.9 Wm^{-2}) and high interannual monthly class albedo variability (3.9% for $v_{\text{ecoregion, 1973}}$ and $v_{\text{ecoregion, 200}}$) that is perhaps associated with variable vegetation response to rainfall in the near desert conditions. For all but 2 of the 45 ecoregions, the vertical error bar lines intersect the zero surface radiative forcing horizontal line. Only ecoregion 2 (Puget Lowland) and ecoregion 33 (East Central Texas Plains) have unambiguous cooling and forcing estimates, respectively. Evidently, the ecoregion annual surface radiative forcing estimates are highly sensitive to interannual albedo variability.

[41] At the CONUS scale for the 45 ecoregions, we estimate a snow-free net surface radiative forcing of 0.043 Wm^{-2} due to LCLU albedo change from 1973 to 2000 equation (11) with an error of 0.084 Wm^{-2} equation (15). This net surface radiative forcing error is very high and illustrates the ecoregion annual surface radiative forcing estimates are very sensitive to interannual albedo variability.

5. Conclusion

[42] The monthly variation of albedo, snow cover, and incoming surface solar radiation were used to (1) quantify the surface radiative forcing due to contemporary (1973–2000) LCLU albedo change for 69% of the CONUS, (2) analyze the impact of modeling snow conditions on surface radiative forcing, and (3) determine the sensitivity of surface radiative forcing to interannual albedo variation.

[43] Across the CONUS, agricultural land use has been in decline [*Drummond and Loveland*, 2010] and the rates of forest harvesting [*Pinder et al.*, 1999] and ex-urban sprawl have been accelerating [*Brown et al.*, 2005; *Steyaert and Knox*, 2008]. For the 58 CONUS ecoregions considered, the dominant contemporary LCLU changes from 1973 to 2000 documented by the USGS Land Cover Trends Project data were a net areal decrease in agricultural land (−1.3%) and forest (−0.9%) and a net increase in developed (1.2%) and grass/shrub (0.7%). The most extensive LCLU changes occurred in the Pacific Northwest (>25%) and in the Southeast (>20%) and the least (<1%) in the desert southwest.

[44] Nine years of MODIS albedo data were used to extract, for each ecoregion and month, the median broadband white-sky snow and snow-free albedos for each of ten LCLU classes defined by the USGS Land Cover Trends data set. The snow and snow-free albedo class values were broadly comparable to other worker's results [*Jin et al.*, 2002; *Gao et al.*, 2005]. The median monthly LCLU class albedos were used to compute ecoregion specific albedo estimates independently for years 1973 and 2000.

[45] It is established that snow has a significant land cover-dependent albedo and radiative forcing effect [*Betts*, 2000]. In this study approximately two thirds of the 58 CONUS ecoregions had significant mean annual snow cover. However, the net CONUS surface radiative forcing only changed by 0.003 Wm^{-2} when snow and snow-free conditions were modeled over the 58 ecoregions. The extent of the LCLU change, the snow and snow-free albedos of the LCLU change classes, and the monthly snow fraction determined the surface radiative forcing. In snow-prone ecoregions where the dominant LCLU transitions were between snow-hiding and snow-revealing LCLU classes both the negative and positive ecoregion forcings were amplified. This snow/snow-free difference was most significant in the Sierra Nevada ecoregion where the surface radiative forcing modeling snow conditions was 0.207 Wm^{-2} more negative than when snow was not modeled, due to high winter monthly snow fractions (between 0.57 and 0.73) and a primary 1973–2000 LCLU transition from

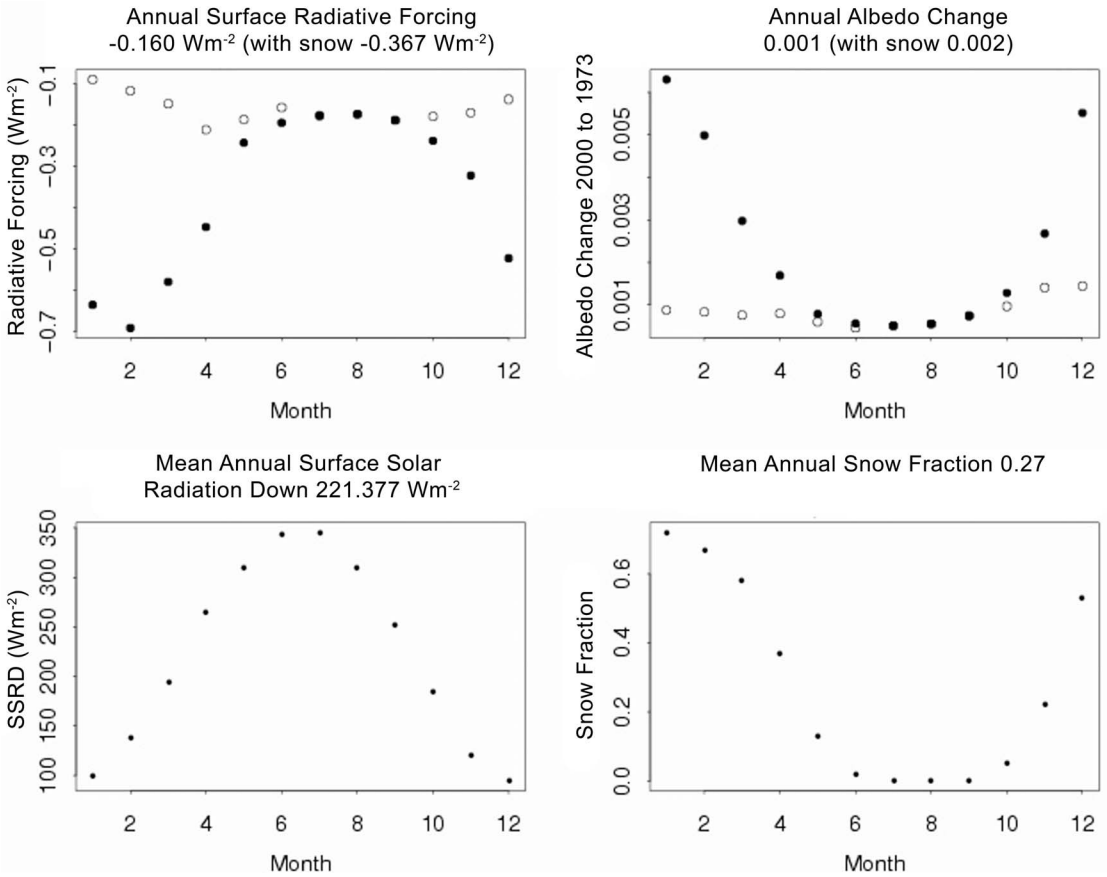

Figure 9. Ecoregion 5 (Sierra Nevada) monthly variability in surface radiative forcing, 1973–2000 LCLU albedo change, surface solar radiation and snow fraction. The monthly surface radiative forcing and albedo change estimates modeling snow (black circles) and snow-free (white circles) conditions are shown.

forest (snow-hiding) to nonmechanically disturbed (snow-revealing) classes.

[46] The monthly interannual albedo variability over 9 years of MODIS data was used to examine the sensitivity of the contemporary LCLU albedo change radiative forcing estimates. Only the interannual variability for 45 of the 58 ecoregions with sufficient snow-free MODIS albedo observations to compute the MAD statistic was quantified. The ecoregion percent average monthly variation in snow-free albedo ranged from 1.6% to 4.3% across the 45 ecoregions. This interannual albedo variability and the magnitude of the incoming surface solar radiation determined the ecoregion surface radiative forcing errors, which were large, from 0.138 Wm^{-2} to 0.842 Wm^{-2}. For the 45 ecoregions considered, a CONUS snow-free net surface radiative forcing of 0.044 Wm^{-2} with a relatively large error of 0.084 Wm^{-2} was estimated.

[47] At the CONUS scale, for the 58 ecoregions considered, we estimated a net positive (i.e., warming) surface radiative forcing of 0.029 Wm^{-2} due to contemporary LCLU albedo change. Similarly, a recent study on the impact of CONUS LCLU change on surface temperature indicated that LCLU changes often resulted in more warming than cooling [*Fall et al.*, 2009]. The surface radiative forcing varied in sign and magnitude among the 58 ecoregions, with the transition to forest causing the most negative forcing (−0.367 Wm^{-2}), and the conversion to grass/shrub causing the most positive forcing (0.337 Wm^{-2}). This magnitude of ecoregion scale forcing is similar to global LCLU change forcing estimates since 1750 [*IPCC*, 2007]. The surface radiative forcing of 0.029 Wm^{-2} is greater than our earlier 0.012 Wm^{-2} reported estimate [*Barnes and Roy*, 2008] as 26% more area of the CONUS was considered and because we modeled snow conditions.

[48] The research reported in this paper underscores the value of spatially and temporally explicit data to quantify, and begin to understand, LCLU albedo change-related surface radiative forcing. However, our analysis illustrates, as observed by previous studies [*Pielke et al.*, 2002; *National Research Council*, 2005; *IPCC*, 2007], that the radiative forcing of LCLU albedo change remains uncertain. The need to improve and accurately represent LCLU and other surface characteristics including albedo is clear. The MODIS satellite-derived albedo product used in this study is a significant improvement on previous model and scenario-based albedo estimates [*Betts*, 2000; *Roesch et al.*, 2002], but there is potential for improved spatially and temporally explicit albedo by calibration with land surface model outputs [*Matsui et al.*, 2007]. Improved continental incoming solar radiation data may also provide more reliable forcing

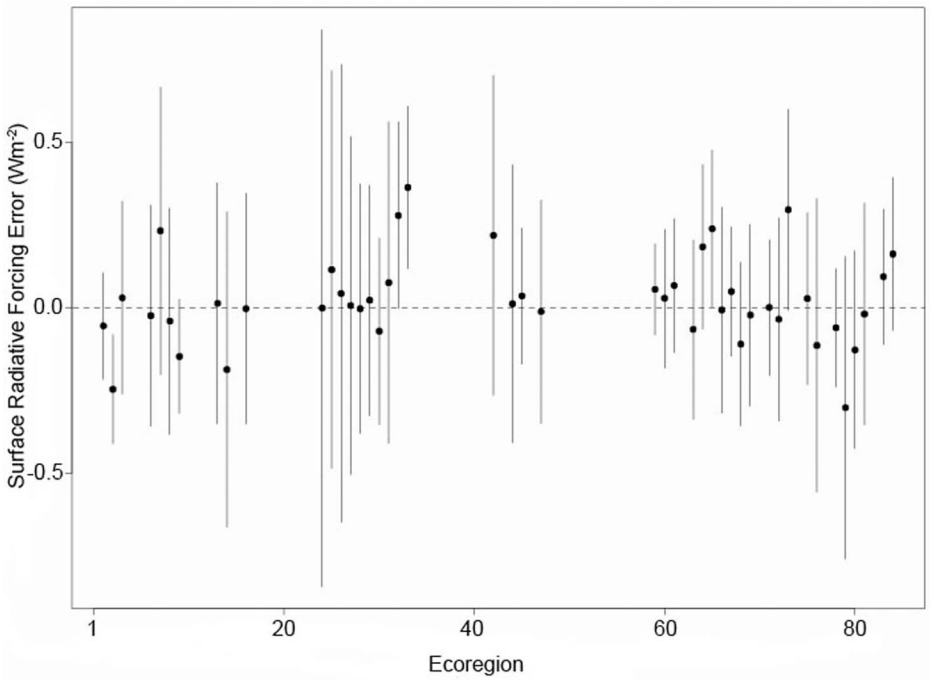

Figure 10. Ecoregion snow-free annual surface radiative forcing due to contemporary land cover land use albedo change from 1973 to 2000 (black circles) equation (10) ± the annual surface radiative forcing error imposed by inter-annual albedo variability (vertical lines) equation (14). Only snow-free forcing results for 45 of the 58 ecoregions considered in this study are illustrated.

estimates. For example, the North American Regional Reanalysis data set was recently reprocessed [*Mesinger et al.*, 2006] and is defined with 32 km grid cells that will capture spatial variability in incoming solar radiation more precisely than the ERA-40 data used in this study. Further research will be undertaken building on these new data sets and using a greater number of CONUS ecoregion LCLU data sets as they become available from the USGS Land Cover Trends Project.

[49] **Acknowledgments.** This work was funded by NASA grant NNX06AF87H. We gratefully acknowledge the USGS Land Cover Trends Project for access to their data. The Collection 5 NASA MODIS albedo and snow fraction data are available from the USGS EROS and the National Snow and Ice Data Centers respectively. The ERA-40 data were provided by the European Center for Medium-Range Weather Forecasts. We acknowledge the useful comments made by the reviewers.

References

Allan, R. P., M. A. Ringer, J. A. Pamment, and A. Slingo (2004), Simulation of the Earth's radiation budget by the European Centre for Medium-Range Weather Forecasts 40-year reanalysis (ERA40), *J. Geophys. Res.*, *109*, D18107, doi:10.1029/2004JD004816.

Barnes, C. A., and D. P. Roy (2008), Radiative forcing over the conterminous United States due to contemporary land cover land use albedo change, *Geophys. Res. Lett.*, *35*, L09706, doi:10.1029/2008GL033567.

Betts, A. K., and J. H. Ball (1997), Albedo over the boreal forest, *J. Geophys. Res.*, *102*(D24), 28,901–28,909, doi:10.1029/96JD03876.

Betts, R. A. (2000), Offset of the potential carbon sink from boreal forestation by decreases in surface albedo, *Nature*, *408*, 187–190.

Brown, D. G., K. M. Johnson, T. R. Loveland, and D. M. Theobald (2005), Rural land use trends in the conterminous United States, 1950–2000, *Ecol. Appl.*, *15*, 1851–1863.

Dickinson, R. E. (1995), Land processes in climate models, *Remote Sens. Environ.*, *51*, 27–38.

Drummond, M. A., and T. R. Loveland (2010), Land-use pressure and a transition to forest-cover loss in the Eastern United States, *BioScience*, *60*, 286–298.

Fall, S., D. Niyogi, A. Gluhovsky, R. A. Pielke Sr., E. Kalnay, and G. Rochon (2009), Impacts of land use land cover on temperature trends over the continental United States: Assessment using the North American Regional Reanalysis, *Int. J. Climatol.*, doi:10.1002/joc.1996.

Gao, F., C. B. Schaaf, A. H. Strahler, A. Roesch, W. Lucht, and R. Dickinson (2005), MODIS bidirectional reflectance distribution function and albedo Climate Modeling Grid products and the variability of albedo for major global vegetation types, *J. Geophys. Res.*, *110*, D01104, doi:10.1029/2004JD005190.

Gibbard, S., K. Caldeira, G. Bala, T. J. Philips, and M. Wickett (2005), Climate effects of global land cover change, *Geophys. Res. Lett.*, *32*, L23705, doi:10.1029/2005GL024550.

Hall, D. K., and G. A. Riggs (2007), Accuracy assessment of the MODIS snow-cover products, *Hydrol. Process.*, *21*(12), 1534–1547, doi:10.1002/hyp.6715.

Hall, D. K., G. A. Riggs, and V. V. Salomonson (2006), updated monthly. MODIS/Terra Snow Cover Monthly L3 Global 0.05Deg CMG V005, [Dates used; January 2004 to December 2008]. Boulder, Colorado USA: National Snow and Ice Data Center. Digital media.

Intergovernmental Panel on Climate Change (IPCC) (2007), *Climate Change 2007: The Physical Science Basis, Contribution of Working Group I to the Fourth Assessment Report of the Intergovernmental Panel on Climate Change*, edited by S. Solomon et al., 996 pp., Cambridge Univ. Press, New York.

Jin, Y., and D. P. Roy (2005), Fire-induced albedo change and its radiative forcing at the surface in northern Australia, *Geophys. Res. Lett.*, *32*, L13401, doi:10.1029/2005GL022822.

Jin, Y., C. B. Schaaf, F. Gao, X. Li, A. H. Strahler, X. Zeng, and R. E. Dickinson (2002), How does snow impact the albedo of vegetated land surfaces as analyzed with MODIS data?, *Geophys. Res. Lett.*, *29*(10), 1374, doi:10.1029/2001GL014132.

Johnson, J., and B. Maxwell (2001), The role of the Conservation Reserve Program in controlling rural residential development, *J. Rural Stud.*, *17*, 323–332.

Kleidon, A. (2006), The climate sensitivity to human appropriation of vegetation productivity and its thermodynamic characterization, *Global Planet. Change*, *54*, 109–127.

Loveland, T. R., and W. Acevedo (2010), Land cover change in the Eastern United States, in *Status and Trends of Eastern United States Land Cover*, edited by W. Acevedo and P. J. Jellison, U.S. Geol. Surv. Prof. Pa., in press.

Loveland, T. R., T. L. Sohl, S. V. Stehman, A. L. Gallant, K. L. Sayler, and D. E. Napton (2002), A strategy for estimating the rates of recent united states land cover changes, *Photogramm. Eng. Remote Sens.*, *68*(10), 1091–1099.

Matsui, T., A. Beltran-Przekurat, R. A. Pielke Sr., D. Niyogi, and M. Coughenour (2007), Continental-scale multi-objective calibration and assessment of Colorado State University Unified Land Model: Part I. Surface albedo, *J. Geophys. Res.*, *112*, G02028, doi:10.1029/2006JG000229.

Mesinger, F., et al. (2006), North American regional reanalysis: A long-term, consistent, high-resolution climate data set for the North American domain, as a major improvement upon the earlier global reanalysis data sets in both resolution and accuracy, *Bull. Am. Meteorol. Soc.*, *87*, 343–360.

Myhre, G., and A. Myhre (2003), Uncertainties in radiative forcing due to surface albedo changes caused by land-use changes, *Am. Meteorol. Soc.*, *16*(10), 1511–1524.

Nair, U. S., D. K. Ray, J. Wang, S. A. Christopher, T. Lyons, R. M. Welch, and R. A. Pielke Sr. (2007), Observational estimates of radiative forcing due to land use change in southwest Australia, *J. Geophys. Res.*, *112*, D09117, doi:10.1029/2006JD007505.

National Research Council (2005), *Radiative Forcing of Climate Change: Expanding the Concept and Addressing Uncertainties*, 207 pp., Natl. Acad., Washington, D. C.

Omernik, J. M. (1987), Ecoregions of the conterminous United States, *Annu. Assoc. Am. Geogr.*, *77*, 118–125.

Pielke, R. A., G. Marland, R. A. Betts, T. N. Chase, J. L. Eastman, J. O. Niles, D. S. Niyogi, and S. W. Running (2002), The influence of land-use change and landscape dynamics on the climate system—Relevance to climate change policy beyond the radioactive effect of greenhouse gases, *Phil. Trans. R. Soc. Ser. A.*, *360*, 1705–1719.

Pinder, J. E., III, T. E. Rea, and D. E. Funsch (1999), Deforestation, reforestation, and forest fragmentation on the upper coastal plain of South Carolina and Georgia, *Am. Midland Naturalist*, *142*, 213–228.

Ramankutty, N., and J. A. Foley (1999), Estimating historical changes in global landcover: croplands from 1700 to 1992, *Global Biogeochem. Cycles*, *13*(4), 997–1027, doi:10.1029/1999GB900046.

Roesch, A., M. Wild, R. Pinker, and A. Ohmura (2002), Comparison of spectral surface albedos and their impact on the general circulation model simulated surface climate, *J. Geophys. Res.*, *107*(D14), 4221, doi:10.1029/2001JD000809.

Román, M. O., C. B. Schaaf, P. Lewis, F. Gao, G. P. Anderson, J. L. Privette, A. H. Strahler, C. E. Woodcock, and M. Barnsley (2009), The MODIS (Collection V005) BRDF/albedo product: Assessment of spatial representativeness over forested landscapes, *Remote Sens. Environ.*, *113*, 2476–2498.

Schaaf, C. B., et al. (2002), First Operational BRDF, albedo and nadir reflectance products from MODIS, *Remote Sens. Environ.*, *83*(1–2), 135–148.

Schaaf, C. L., J. Martonchik, B. Pinty, Y. Govaerts, F. Gao, A. Lattanzio, J. Liu, A. H. Strahler, and M. Taberner (2008), Retrieval of surface albedo from satellite sensors, in *Advances in Land Remote Sensing: System, Modeling, Inversion and Application*, edited by S. Liang, pp. 219–243, Springer, ISBN 978-1-4020-6449-4.

Serra, J. (1982), *Image Analysis and Mathematical Morphology*, Academic, London.

Stehman, S. V., T. L. Sohl, and T. R. Loveland (2005), An evaluation of sampling strategies to improve precision of estimates of gross change in land use and land cover, *Int. J. Remote. Sens.*, *26*, 4941–4957.

Steyaert, L. T., and R. G. Knox (2008), Reconstructed historical land cover and biophysical parameters for studies of land-atmosphere interactions within the eastern United States, *J. Geophys. Res.*, *113*, D02101, doi:10.1029/2006JD008277.

Uppala, S. M., et al. (2005), ERA-40 re-analysis, *Q. J. R. Meteorol. Soc.*, *131*, 2961–3012, doi:10.1256/qj.04.176.

Wang, S., and A. Davidson (2007), Impact of climate variations on surface albedo of a temperate grassland, *Agric. Forest Meterol.*, *142*, 133–142.

Wang, Z., X. Zeng, M. Barlage, R. E. Dickinson, F. Gao, and C. Schaaf (2004), Using MODIS BRDF and albedo data to evaluate global model land surface albedo, *J. Hydrometeorol.*, *5*, 3–14.

Zhou, L., et al. (2003), Comparison of seasonal and spatial variations of albedos from Moderate-Resolution Imaging Spectroradiometer (MODIS) and Common Land Model, *J. Geophys. Res.*, *108*(D15), 4488, doi:10.1029/2002JD003326.

C. A. Barnes and D. P. Roy, Geographical Information Science Center of Excellence, South Dakota State University, Brookings, SD 57007, USA. (christopher.barnes@sdstate.edu; david.roy@sdstate.edu)